PAPER • **OPEN ACCESS**

Design and identification of an optimal approach for modelling a hybrid renewable energy system

To cite this article: Are Parameswarudu *et al* 2025 *Eng. Res. Express* **7** 045350

Engineering Research Express

OPEN ACCESS

RECEIVED
27 June 2025

REVISED
2 October 2025

ACCEPTED FOR PUBLICATION
17 October 2025

PUBLISHED
6 November 2025

PAPER

Design and identification of an optimal approach for modelling a hybrid renewable energy system

Are Parameswarudu[1], **Yadala Pavankumar**[2,*], **Patibandla Anilkumar**[3] and **Ravindra Kollu**[4]

[1] Department of Electrical Engineering, National Institute of Technology, Tadepalligudem, India
[2] School of Electronics and Computer Science, University of Southampton, Southampton, United Kingdom
[3] School of Electronic Science and Engineering, University of Electronic Science and Technology of China, People's Republic of China
[4] Department of Electrical and Electronics Engineering, University College of Engineering Kakinada, Jawaharlal Nehru Technological University Kakinada, India
[*] Author to whom any correspondence should be addressed.

E-mail: p.k.yadala@soton.ac.uk

Keywords: renewable energy sources, photovoltaic, biomass, deterministic approach, loss of power supply probability, probabilistic approach, multi-objective optimization

Supplementary material for this article is available online

Abstract

Most power generation relies on fossil fuels, which are both finite resources and major contributors to greenhouse gas emissions. In recent years, renewable energy sources such as solar, wind, and biomass have played an important role in power generation to mitigate these concerns. However, the successful modelling, operation, and integration of these sources into the grid system poses significant challenges due to their inherent variability and dependency on environmental conditions. Due to these challenges, determining the optimal capacity of renewables in a hybrid system is complex. Thus, a robust methodology is required to address this design challenge effectively. To achieve this, development of advanced modelling techniques is suggested that consider the probabilistic nature of renewable energy sources and load patterns. This study analyses different approaches, including the deterministic and probabilistic methods, and proposes an optimal approach and design for a hybrid renewable energy system, which is more reliable with a reduced loss of power supply probability and produces energy with 26.3% lower levelised cost of electricity (LCOE) than fossil fuel–based alternatives such as the utility grid. A detailed analysis of the compatibility of the proposed method with the actual real-time data is carried out, and the effect of the grid purchase and sale capacities on the LCOE of the produced energy is examined.

1. Introduction

The electricity sector in India is undergoing a significant transformation. As of 2024, India's total installed power generation capacity stands at approximately 452.7 GW [1]. However, reliance on traditional (non-renewable) sources like coal is continually declining. Although fossil fuels currently account for approximately 55.5% of total energy capacity, their dominance is progressively declining owing to sustainability concerns, environmental impacts, and economic drawbacks [2]. Therefore, a shift towards renewable energy sources is not just desirable, but necessary. On the other hand, renewable energy sources like hydro-power, wind, and solar are on the rise, contributing approximately 44.5% of the total installed capacity. With a predominantly agrarian economy supporting much of its population, India generates approximately 228 million tons of agricultural waste annually. This untapped resource has the potential to generate approximately 11.32 GW of power, offering a significant opportunity to enhance renewable energy production [3]. The use of this agricultural waste for generating electrical power would decrease the burden on conventional means.

Renewable energy sources such as solar and wind are intermittent, meaning their generation varies based on weather conditions and stochastic nature [4]. This unpredictability makes them dependent on external

factors, leading to inconsistent energy production. Such variability presents challenges for grid stability and a consistent power supply. The use of hybrid renewable energy systems (HRESs) can address this issue [5]. However, integrating these variable renewable energy sources into the power grid presents several challenges, like power management issues, decreased reliability, and grid instability. To address these challenges, HRES that combine with energy storage systems (ESS) are gaining traction [6]. HRES offers a promising solution for reliable and sustainable power generation. However, determining the optimal design of HRES is essential to ensure economic viability, meet power demand, and maintain grid stability.

Numerous studies over the past few decades have focused on the optimal sizing of standalone HRES [7–10]. Suhane *et al* [11] in 2016 have proposed wind, photovoltaic (PV) off-grid HRES by considering the hourly meteorological data per year. The optimisation has been carried out by ant colony optimisation algorithm to optimise the energy cost and unmet load. In 2020, Hadi Razmi *et al* [12] modelled the standalone HRES with wind, fuel cell, electrolyser, hydrogen tank, and biomass. Various optimisation algorithms have been used to find the optimal sizing of HRES and to reduce the power supply cost per unit. In 2023, Menesy *et al* [13] presented the optimisation of grid-independent HRES with solar, wind, biomass, and hydro-pumped storage using the heap-based optimiser by using the yearly data. The goal of the optimisation is to reduce the total energy cost and to minimise the loss of power supply probability. The results are validated with the grey wolf optimiser (GWO) and particle swarm optimisation (PSO). Yemeli *et al* [14] in 2024 proposed off-grid HRES with solar, wind, diesel, and fuel cell for optimal sizing using various evolutionary algorithms. The optimisation objective is to minimise the cost of energy (COE), subject to the reliability constraint of maintaining the loss of power supply probability (LPSP) within acceptable limits. Different scenarios are considered based on the load requirements, and various hybrid systems are compared.

The reliability of the power system can be improved by integrating the hybrid renewable energy system (HRES) into the grid. However, this integration poses challenges due to the variable and stochastic nature of renewable energy sources (RES), which can lead to issues such as frequency deviations, load mismatches, and voltage instability [15, 16]. As a result, energy storage systems have become crucial for the successful grid integration of hybrid renewable energy sources [17–19]. In 2017, Basaran *et al* [20] developed a grid-integrated system with a PV, wind, and battery-based renewable system, considering cost optimisation and reliability, but not the energy transfer aspects. Kutaiba *et al* [21] proposed an HRES aimed at minimising its cost using a fuzzy logic - GWO technique. However, the modelling of the system is not adequately addressed. The objective of cost minimisation and reliability maximisation for a system designed with PV, battery, and grid integration was addressed in references [22, 23]. However, the variable nature of the energy sources and load was not thoroughly considered. In 2023, Chinna *et al* [24] proposed a grid-integrated HRES with PV, wind, a diesel generator, and a battery storage system. Using the HOMER with yearly data of renewable sources, they have carried out a techno-economic and environmental analysis to construct the optimal system. A similar approach is proposed in [25] with HOMER and analyses the effects of CO, CO_2 and NO_2 on Putrajaya city. But, variable nature of the renewables or load is not considered. B.K.Reddy, *et al* [26] developed an approach for the optimal operation of the cogeneration power plant, which is integrated with solar. The method uses the batteries to support the critical loads, but the dependency on the renewable energy is minimal. To design the renewable power-generation technologies with consideration of the intermittent and stochastic nature of the sources, PDFs are required [27, 28]. The PDFs were utilised in [29, 30] to characterise the variable nature of the sources, load, and power production. However, proper system modelling was overlooked.

Conventional HRES design approaches often fail to account for the probabilistic nature of RES and load variations, resulting in sub-optimal system configurations that may not effectively address reliability concerns or minimise costs. Additionally, utilising bio-waste for electricity generation can help reduce the loss of power supply [31]. Furthermore, battery storage becomes crucial in managing these variations and ensuring grid stability.

Designing a reliable grid-integrated HRES requires robust mathematical modelling to address the stochastic and intermittent nature of renewable resources. While deterministic simulations using annual data are common, they can be computationally intensive and fail to explicitly model the underlying stochastic nature of generation. This study introduces a probabilistic framework using Probability Density Functions (PDFs) to characterize variability using statistical data, specifically comparing the efficacy of monthly versus seasonal models for optimizing reliability and cost. This provides a streamlined, complementary design tool. Additionally, existing optimal HRES designs often overlook biomass integration, a stable and dispatchable resource that could significantly improve system reliability. Based on the above literature, this study proposes a dedicated approach for the optimal design of grid-integrated HRES that incorporates a probabilistic framework to reduce the Levelised Cost of Electricity (LCOE) from annual life cycle costing (ALCC) and LPSP. The Harmony Search Algorithm (HSA) is employed to solve the optimisation problem, and the impact of the grid partitioning factor is analysed.

The major contributions of this work are as follows:

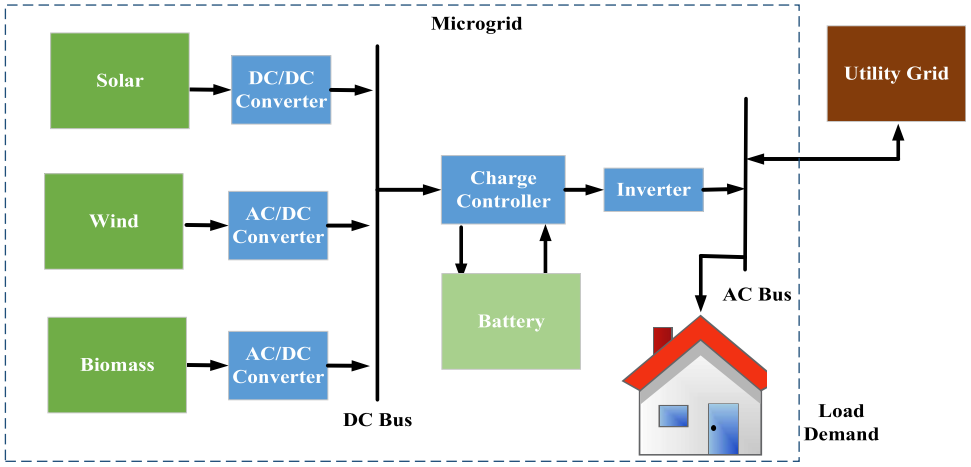

Figure 1. Schematic diagram of Grid-integrated Hybrid renewable energy system.

1. Finding the optimal combination of HRES with a deterministic approach, used historically in the literature, which minimises both the LCOE and the LPSP using HSA;
2. Applying various PDFs on the solar, wind, and load profiles to identify a suitable PDF to model the HRES, considering both monthly and seasonal variations;
3. Integrating the probabilistic models with a multi-objective metaheuristic algorithm to design HRES with a monthly and seasonal approach;
4. Detailed and robust analysis of both approaches, and identification of the optimal approach with real-time data validation.

2. Modelling of a hybrid renewable energy system

Figure 1 shows the schematic diagram of grid-integrated HRES, including the renewable sources like solar, wind, and biomass. To optimise the design of this HRES integrating solar, wind, biomass, energy storage, and grid connectivity, precise modelling of both energy generation and load demand is crucial, though challenging due to the dependency of renewable sources on varying environmental conditions. This section focuses on two complementary modelling approaches: a deterministic model assesses the performance of various combinations of renewable sources, while a probabilistic model incorporates the time-varying and stochastic behaviour of renewable energy sources in the design process of HRES.

2.1. Deterministic modelling

For this study, the meteorological data (irradiance, temperature, and wind speed) are collected at Gangadevipalli village (latitude-4°34′24.1 E and longitude –78°19′44.9 N), which is nearly 120 km from Kadapa, Andhra Pradesh, India. Load demand data is recorded at the local substation, revealing a peak load of 100 kW and an average load of approximately 50 kW. The collected meteorological data (irradiance, temperature, and wind speed) over four years are averaged to obtain the final set of data for the deterministic approach.

2.1.1. Solar PV system modelling

The output of a solar PV panel depends mainly on atmospheric conditions and geographical locations. The output power of a particular solar PV panel (P_{pv}), at any time 't' is a function of solar irradiance and atmospheric temperature, and it is expressed as follows:

$$P_{pv}(t) = f_{pv} \cdot N_{pv} \cdot \eta_{mppt} \cdot I_{sc}(t) \cdot V_{oc}(t).ff \quad (1)$$

where, ff is a fill factor, f_{pv} is derating factor, η_{mppt} is mppt factor, N_{pv} is the number of PV modules and the short circuit current (I_{sc}) and open circuit voltage (V_{oc}) are given in equations (2)–(3).

$$I_{sc}(t) = I_{stc} + k_i \cdot (T_{cell}(t) - T_{stc}) \cdot (s(t)/s_{stc}) \quad (2)$$

$$V_{oc}(t) = V_{stc} + k_v \cdot (T_{cell}(t) - T_{stc}) \quad (3)$$

where k_v and k_i represent the voltage and current coefficients of the temperature, T_{stc} is the module temperature at STC, s is the hourly solar radiation incident on the solar PV panel (W m^{-2}), s_{stc} is the standard incident

radiation (1000 W m^{-2}), T_{cell} is the cell temperature, and V_{stc} and I_{stc} are the voltage and current at STC, respectively.

2.1.2. Wind energy system modelling

Wind turbine power production is a function of time-variant wind velocity, exhibiting stochastic variability due to changing atmospheric conditions. Therefore, wind turbine output power at any time frame '*t*' (hour) can be given by equation (4).

$$Pwt(t) = \begin{cases} P_{rw} \cdot N_w \cdot \left(\dfrac{v(t) - v_{ci}}{v_r - v_{ci}}\right) & for\ v_{ci} < v(t) < v_r \\ P_{rw} \cdot N_w & for\ v_r < v(t) < v_{co} \\ 0 & else \end{cases} \tag{4}$$

where N_w is number of wind turbines, P_{rw} is rated power of the wind turbine (kW), $v(t)$ represents the wind velocity (m/s) at time '*t*', v_{ci} is the cut-in velocity (m/s), v_{co} is the cut-out velocity (m/s), and v_r is the rated velocity (m/s).

2.1.3. Biomass gasifier modelling

The biomass gasifier generates electricity through thermochemical conversion of feedstock via oxygen-limited gasification. The resulting syngas fuels a generator to produce power. For this case study, we analysed a 10 kW gasifier system operating 12 h daily, primarily during peak demand periods. The total annual biomass energy (E_{bio}) generated is given in the following equation:

$$E_{bio} = P_{bio} * t_{bio} * N_{bio} \tag{5}$$

where N_{bio} is the total number of biomass gasifiers, P_{bio} is the biomass gasifier output power, and t_{bio} is operating hours per year. The maximum gasifier capacity depends on the total available biomass, its calorific value (CV_{bm} in kWh/ton), and the biomass gasifier conversion efficiency (η_{bio}).

$$P_{bio}^{max} = \frac{CV_{bm} * 1000 * total_{agriwaste} * \eta bio}{t_{bio} * 8760 * 365} \tag{6}$$

2.1.4. Battery energy storage system modelling

For this study, lead-acid batteries are considered because of their low capital cost, high cycle efficiency (70%–85%), and low self-discharge rate (3%–20%). The battery energy storage system (BESS) provides critical peak shaving capability, delivering a minimum of 30 min of backup power during load peaks. During periods of high demand or renewable generation shortfalls, the system prioritises battery dispatch to maintain grid stability. During periods of renewable generation surplus, excess energy is directed to charge the batteries. The state of charge (SOC) of the battery determines the amount of energy stored in the battery. During charging mode, the state of charge (SOC) is given by equation (7).

$$SOC(t+1) = SOC(t) + \frac{I_{bat}(t) * \Delta t}{C_{bat}} \tag{7}$$

The actual SOC of the battery is always less than the original SOC because of the self-discharging rate (s_{dr}) of the battery, and the charge efficiency factor (η_c). The actual SOC can be expressed in equation (8) as follows:

$$SOC(t+1) = SOC(t) \cdot (1 - sdr) + \frac{I_{bat}(t) \cdot \Delta t \cdot \eta_c(t)}{C_{bat}} \tag{8}$$

where Δt is the time step. The charge efficiency factor is given by the following equation:

$$\eta_c(t) = 1 - \exp\left[\frac{a \cdot (SOC(t) - 1)}{I_{bat}(t)/I_{10} + b}\right] \tag{9}$$

where the parameters a, b, I_{10} are considered as 20.73, 0.55, and 10, respectively, and C_{bat} is the battery nominal capacity (Ah). At any time t, the charging current ($I_{bat}(t)$) during charging mode is given as follows:

$$I_{bat}(t) = \frac{(P_{pv}(t) + P_{wt}(t) \cdot \eta_{re} + N_{bio} P_{bio}(t) \cdot \eta_{re}) - (P_l(t)/\eta_{in})}{Nb_{st} \cdot Nb_{se} \cdot V_{bat}} \tag{10}$$

$$Nb_{st} = \frac{(P_l) * 0.5}{Nb_{se} \cdot \quad V_{bat} \cdot I_{bat,\max}} \tag{11}$$

where N_{bse} is the number of series-connected batteries, V_{bat} is the battery terminal voltage, η_r and η_i are the efficiencies of the rectifier and inverter, respectively.

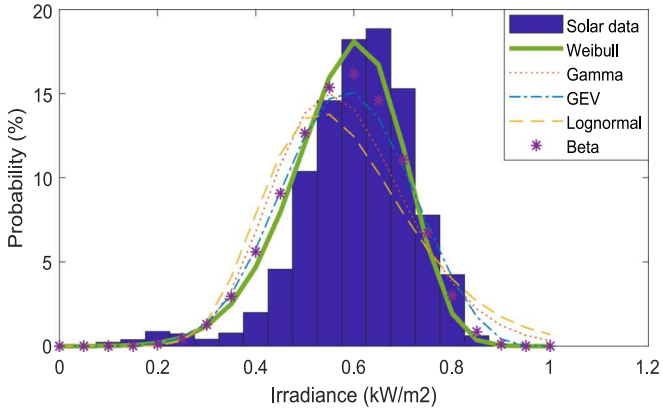

Figure 2. Curve fitting for the solar irradiance data with various PDFs.

The SOC of the BESS during the discharging process is given by the following equation:

$$SOC(t+1) = SOC(t)^{*}(1 - sdr) - \frac{I_{bat} \cdot \Delta t}{C_{bat}} \tag{12}$$

where I_{bat} during the discharging mode can be given as follows:

$$I_{bat}(t) = \frac{(P_l(t)/\eta_{in}) - (P_{pv}(t) + P_{wt}(t) \cdot \eta_{re} + N_{bio} P_{bio}(t) \cdot \eta_{re})}{Nb_{st} \cdot Nb_{se} \cdot V_{bat}} \tag{13}$$

$$Ibat,\ \max(t) = \max\{0,\ \min[I\ \max, Cbat\ (c_b\ (soc\ \max - soc(t)) + (soc(t) - soc\ \min)\ (1 - c_b))/\Delta t]\} \tag{14}$$

where $SOC_{\max}$ is 1, $SOC_{\min}$ is 30%, $I_{\max}$ is 20% of its nominal capacity of the battery (C_{bat}), and c_b is 1 during charging and 0 during discharging.

2.2. Probabilistic modelling

The probabilistic methodology used in this study models the statistical dependence between solar irradiance, ambient temperature, wind speed, and load demand. This interdependence is critical to the output performance of the system. For example, in the Gangadevipalli location, hot, sunny weather creates a positive correlation, simultaneously increasing solar generation and cooling demand. Consequently, during peak sun hours, solar energy can meet the high concurrent load, reducing the energy purchased from the grid. Any demand exceeding our purchase limit is recorded as an unmet load (LPS). This analysis was achieved by generating correlated data profiles that realistically pair solar output with demand. The considered robust approach demonstrates that simulating real-world correlations provides a more accurate reliability assessment than a deterministic method. At any given sample of time, the probability of the random variable that could fall under a particular range can be determined by using the PDFs. For characterising the variable nature of the renewable energy sources and load, different PDFs are used to fit the wind data, solar irradiance, and load demand. The optimal PDF for each dataset was selected through visual interpretation of the distribution fit, supplemented by quantitative goodness-of-fit metrics, including the coefficient of determination (R^2) and the Kolmogorov-Smirnov (K-S) error.

- R^2 score reflects the correlation between the observed and the cumulative probabilities. With the larger R^2 value, the better the fitness of the PDF.
- K-S represents the maximum error in cumulative distribution functions. With a lower K-S value indicating a better fitting of the PDF.

Figures 2 and 3 demonstrate that the Weibull PDF provides a visibly superior fit for both solar irradiance and wind speed data distributions. This is further supported by the high R^2 values and low K-S errors reported in tables 1 and 2, confirming the robustness of the Weibull fit. For load data, the normal PDF better fits the data distribution, as shown in figure 4 and table 3.

The Weibull distribution is characterized by a dimensionless shape parameter (k), which governs the spread and form of the distribution, and a scale parameter (c) with units matching the measured variable. The scale parameter defines the central tendency of the distribution and scales the timeline, effectively stretching or compressing the curve.

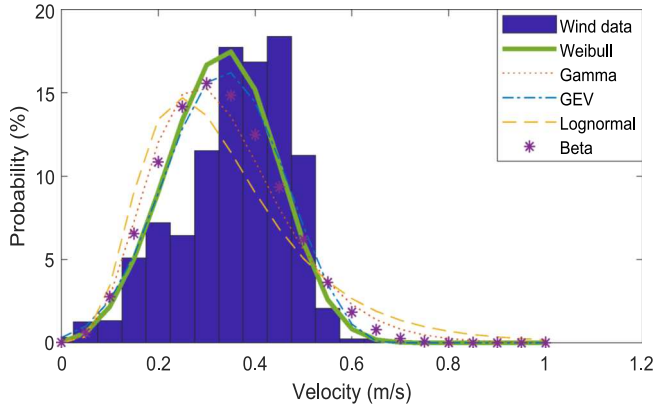

Figure 3. Curve fitting for the wind speed data with various PDFs.

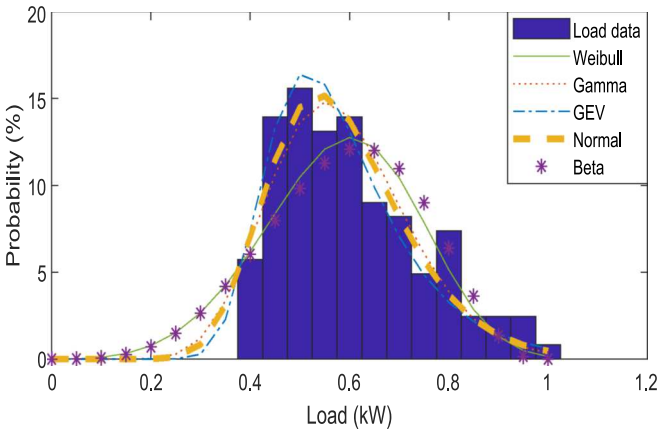

Figure 4. Curve fitting for load data with various PDFs.

Table 1. R^2 and K-S parameters for solar data.

R^2 value	K-S value	PDF
0.9973	0.0388	Weibull
0.9562	0.00823	Gamma
0.9764	0.0665	GEV
0.92268	0.1036	Log normal
0.9831	0.0595	Beta

Table 2. R^2 and K-S parameters for wind data.

R^2 value	K-S value	PDF
0.9974	0.0421	Weibull
0.9733	0.0836	Gamma
0.9967	0.0491	GEV
0.9532	0.1061	Log normal

For the normal distribution, the curve-fitting parameters are μ (mean) and σ (standard deviation), which share the same units as the measured dataset. These parameters are used to determine the probability distribution of the data.

Table 3. R^2 and K-S parameters for load data.

R^2 value	K-S value	PDF
0.9586	0.1810	Weibull
0.9905	0.1694	Normal
0.9800	0.1978	Gamma
0.9730	0.2001	GEV
0.9856	0.1958	Beta

2.2.1. Solar PV system modelling

For any time frame *t*, the scale and shape parameters (c^t) and (k^t), respectively, are determined using the statistical method called maximum likelihood estimation (MLE). The Weibull distribution for the solar irradiance data can be expressed in equation (15) as follows:

$$f(st) = \left(\frac{k^t}{c^t}\right)*\left(\frac{s^t}{c^t}\right)^{k-1}*\exp\left(-\left(\frac{s^t}{c^t}\right)\right)^{k-1} \quad for c^t > 1; k^t > 0 \tag{15}$$

To get the output power from the solar panels, the continuous probability distribution of solar irradiance is split into discrete states for a particular hour '*t*'. Finally, using these probabilities and the power output associated with each irradiance level (state), the average power generation of the solar panel array for that hour can be estimated using equation (16)

$$P_{pv}(t) = \sum_{st=1}^{N} P_{pvst} * P_s(S_{st}^t) \tag{16}$$

The solar irradiance probability for any particular hour is given by,

$$P_s(S_{st}^t) = \begin{cases} \int_0^{\frac{(s_{st}^t + s_{st+1}^t)}{2}} f(s_t)\,ds \text{ for } st = 1 \\ \int_{\frac{(s_{st-1}^t + s_{st}^t)}{2}}^{\frac{(s_{st}^t + s_{st+1}^t)}{2}} f(s_t)\,ds \text{ for } st = 2 \ldots (N_s - 1) \\ \int_{(s_{st-1}^t + s_{st}^t)/2}^{\infty} f(s_t)\,ds \text{ for } st = N_s \end{cases} \tag{17}$$

$$P_{pvst} = N_{pv} * f_{pv} * \eta_{mppt} * ff * I_{sc}(st) * V_{oc}(st) \tag{18}$$

$$ff = (V_{oc} * I_{sc})/(V_{stc} * I_{stc}) \tag{19}$$

The *I*sc and *V*oc can be obtained by the equations (20)–(22),

$$I_{sc}(st) = I_{stc} + k_i * \left(\frac{s_{st}^t}{s_{stc}}\right) * (T_{cell}(st) - T_{stc}) \tag{20}$$

$$V_{oc}(st) = (T_{cell}(st) - T_{stc}) * (V_{stc} + k_v) \tag{21}$$

$$T_{cell}(st) = T_a + \left(\frac{s}{s_{stc}}\right) * (T_{Noct} - T_{aNoct}) \tag{22}$$

2.2.2. Wind energy system modelling

For a given time period '*t*', the wind speed '*v*' (in m/s) is modelled by the Weibull PDF, given by:

$$f(vt) = \left(\frac{k^t}{c^t}\right) * \left(\frac{v^t}{c^t}\right)^{k-1} * \exp^{-\left(\frac{v^t}{c^t}\right)^{k-1}} \tag{23}$$

For any particular time frame '*t*', the average output power is given by equation (24) as follows:

$$P_{wt}(t) = \sum_{st=1}^{N_v} Pwt_{st} \times Pv(v_{st}^t) \tag{24}$$

where the average power in each state and the respective probability can be expressed as below;

$$Pwt_{st} = \begin{cases} P_{rw} * N_w * \left(\dfrac{v_{st}^t - v_{ci}}{v_r - v_{ci}} \right) & for\ v_{ci} < v_{st}^t < v_r \\ P_{rw} * N_w & for\ v_r < v_{st}^t < v_{co} \\ 0 & else \end{cases} \tag{25}$$

$$P_v(v_{st}^t) = \begin{cases} \int_0^{(v_{st}^t + v_{st+1}^t)/2} f(vt)ds\ for\ st = 1 \\ \int_{(v_{st-1}^t + v_{st}^t)/2}^{(v_{st}^t + v_{st+1}^t)/2} f(vt)ds\ for\ st = 2 \ldots (N_v - 1) \\ \int_{(v_{st-1}^t + v_{st}^t)/2}^{\infty} f(vt)ds\ for\ st = N_v \end{cases} \tag{26}$$

2.2.3. Load modelling

For load data, Normal PDF better fits the data distribution. So, for any particular time '*t*', the load demand (KW) is determined as,

$$f(x \mid \mu, \sigma)^2 = \frac{1}{\sqrt{2\pi\sigma^2}} \left(-\frac{(x-\mu)^2}{2\pi\sigma^2} \right) \tag{27}$$

$$P_l(l_{st}^t) = \begin{cases} \int_0^{(l_{st}^t + l_{st+1}^t)/2} f\ (x|\mu, \sigma^2)ds\ for\ st = 1 \\ \int_{\frac{(l_{st-1}^t + l_{st}^t)}{2}}^{\frac{(l_{st}^t + l_{st+1}^t)}{2}} f\ (\mu, \sigma^2)ds\ for\ st = 2 \ldots (N_l - 1) \\ \int_{\frac{(l_{st-1}^t + l_{st}^t)}{2}}^{\infty} f\ (x|\mu, \sigma^2) for\ st = N_l \end{cases} \tag{28}$$

Equation (28) calculates the probability of a specific state, ($P_l(l_{st}^t)$). The load demand for that state is found by multiplying this probability by average load of the state ($P_{l_{st}}$). Therefore, the total average load demand at any time *t* is given by:

$$P_l(t) = \sum_{st=0}^{N_l} P_{l_{st}} * P_l(l_{st}^t) \tag{29}$$

3. Problem formulation

The draining of conventional power sources, exacerbated by growing electricity demand and declining fossil fuel reserves, underscores the critical need for alternative energy systems. This study focuses on the design of a grid-connected HRES to achieve a continuous power supply (low LPSP) at a minimal LCOE. The mathematical models for these objective functions are defined below:

3.1. Annual life cycle cost (ALCC)

For the grid-integrated design of HRES, the overall cost includes the cost of PV, wind turbine, biomass gasifier, battery, and the sale and purchase of power from the grid. Reducing the overall cost reduces the LCOE, therefore the annualised life cycle cost, which can be given as follows:

$$ALCC = \sum_{pv,wind,bat,bio} C_x - C_{gs} + C_{gp} \tag{30}$$

where the component C_x represents the capital, replacement, maintenance, and salvage costs of solar, wind, biomass, and battery of the HRES, and all the costs are annualised, and the detailed description of the same is discussed below. C_{gs} is the cost of the energy sold to the grid, and C_{gp} is the cost of the energy purchased from the grid.

$$C_x = C_x^{am} + C_x^{arp} - C_x^{asg} + C_x^{acap} \tag{31}$$

Here, *x* represents the sources: solar PV/wind/biomass/battery.

3.1.1. Annualised capital cost

For computing the annualized capital cost for any of the component, Net-present value (NPV) is used. The annual capital cost using NPV is given as,

$$C_x^{acap} = C_x^{cap}/NPV \tag{32}$$

where C_x^{cap} is the capital cost of x, and the NPV is given by

$$NPV = \frac{1+f}{1-f}*\left(1-\left(\frac{1+f}{1-i}\right)^n\right) \tag{33}$$

where f, i, and n are the inflation, interest rate, and total lifetime of the project in years, respectively.

3.1.2. Annualised salvage cost

The salvage value refers to the resale or scrap value of a component after the project is complete. For this study, the salvage cost (C_x^{sg}) is considered as 10% of capital cost.

$$C_x^{asg} = C_x^{sg}/NPV \tag{34}$$

3.1.3. Annualised maintenance cost

In the maintenance, running, repair, and other costs are included, which are expressed as follows:

$$C_x^{am} = C_x^{m}*N_x \tag{35}$$

Where N_x is the number of units of a particular component and C_x^m is the maintenance cost of x.

3.1.4. Annualised replacement

Replacement costs are considered for components whose service life is shorter than the project horizon. For this study, the battery bank, with a 5-year lifespan, is the only component requiring replacement; the solar, wind, and biomass assets endure for the project's entire duration. The annualised replacement cost for every replacement is as follows:

$$C_x^{arp} = C_x^{rp}\left(\frac{1+f}{1+i}\right)^n/NPV \tag{36}$$

3.1.5. Energy purchased and sold to grid

In this study, as the design of HRES includes the integration of the grid, the cost of sales and purchase of the power from the grid is also included. The cost of energy purchased is given as follows:

$$C_{gp} = C_g^{p*}\sum_{t=1}^{8760} P_{gp}(t) \tag{37}$$

The total cost of energy sold to grid is given by,

$$C_{gs} = C_g^{p*}\sum_{t=1}^{8760} P_{gs}(t) \tag{38}$$

Finally, the LCOE from the HRES will be given by equation (39) as follows:

$$F_1 = LCOE = \frac{ALCC\left(\frac{Rs}{yr}\right)}{Load\ served\left(\frac{kWh}{yr}\right)} \tag{39}$$

3.2. Loss of power supply probability (LPSP)

The second objective function of this study is to reduce the LPSP, which addresses the reliability of the designed HRES model practically. The mathematical formulation of LPSP is given by,

$$F_2 = LPSP = \frac{\sum_{t=1}^{8760}(P_t^{need} - P_t^{supplied})}{total\ load} \tag{40}$$

and the constrains are

$$\begin{aligned} &N_{pv\_\min} \leqslant N_{pv} \leqslant N_{pv\_\max}, \\ &N_{w\_\min} \leqslant N_{w} \leqslant N_{w\_\max}, \\ &N_{\text{bio}}^{\min} \leqslant N_{bio} \leqslant N_{\text{bio}}^{\max}, \\ &P_{\text{gp}}(t) \leqslant P_{gp}^{\max} P_{gs}(t) \leqslant P_{gs}^{\max} \end{aligned} \tag{41}$$

where *Npv*_min and *Npv*_max are the minimum and maximum number of PV panels, *Nw*_min and *Nw*_max are minimum and maximum number of wind turbines, $N_{bio}^{\min}$ and $N_{bio}^{\max}$ are the minimum and maximum number of biomass gasifiers, and $P_{gp}^{\max}$ and $P_{gs}^{\max}$ are the maximum grid purchase and sale capacity.

4. Operational strategy

4.1. Working strategy

As detailed in section 2.6, the variable nature of solar irradiance, wind speed, and load demand is characterised using Weibull and normal PDFs. This process generates a complete 8760 h annual dataset for each variable. For modelling purposes, this data is decoded into 24 h profiles for 12 typical days (monthly approach, each day represents each month) or 4 typical days (seasonal approach, each day represents each season). It is assumed that the variations within that month or season follow the predicted typical day's 24 h profile, and hence the same variations will be repeated throughout that month or season. The power balance equation of combining the powers from all the sources is given as,

$$\Delta P1(t) = P_{wt}(t)^{*}\eta_{re} + P_{pv}(t) + N_{bio}{}^{*}P_{bio}(t)^{*}\eta_{re} - P_{L}(t)/\eta_{inv} \tag{42}$$

ΔP1 represents the resultant power after meeting the load. If ΔP1 is positive, that represents that the combined power generated from the HRES is more than that of the load demand. Then the remaining power is used to charge the battery until the battery is fully charged. If the battery is fully charged and even then, if power is remaining, then it will be sold to the grid, and as the grid sales and purchase capacities are limited to 18 kW and 10 kW, respectively, to restrict the grid dependency, and if still power remains, it is considered as a dump. The power sold to the grid is given by

$$P_{gs}(t) = (\Delta P1(t) - P_{bat\_c\_\max}(t))^{*}\eta_{inv} \tag{43}$$

If the power generated from the HRES is not able to meet the load demand, then the energy from the battery will be used to meet the load. The deficit power can be expressed as ΔP2.

$$\Delta P2(t) = P_{wt}(t)^{*}\eta_{re} + P_{pv}(t) + N_{bio}{}^{*}P_{bio}(t)^{*}\eta_{re} + I_{bat.\max}{}^{*}V_{bat}{}^{*}N_{b} - P_{L}(t)/\eta_{inv} \tag{44}$$

If the ΔP2 is higher than the available power in the battery, then power will be purchased from the grid. The equation that represents the grid purchase is given as,

$$P_{gp}(t) = P_{L}(t) - (P_{wt}(t)^{*}\eta_{re} + P_{pv}(t) + N_{bio}{}^{*}P_{bio}(t)^{*}\eta_{re} + P_{bat\_c\_\max}(t)^{*}\eta_{inv}) \tag{45}$$

When grid supply capacity is insufficient to meet the demand even after procuring available power, the resulting deficit is treated as unmet load, contributing to the LPSP.

4.2. Multi-objective function

This study employs two objective functions (lowest LPSP and LCOE), which are combined into a single function using the conventional weighted sum approach (WSA), as defined in equation (46). This conventional multi-objective optimisation strategy assigns a weighting factor to each function. Since each objective was deemed equally critical for this study, equal weights were applied.

$$minimise f(x) = \sum_{k=1}^{m} (w_k{}^{*}f_k(x)) \tag{46}$$

where $w_k = 0.5$ since $\sum_{k=1}^{m}(w_k) = 1$. And since f_1 and f_2 are in different ranges, f_1 is normalised as f_1=LCOE/grid cost, which always varies between 0–1 as grid cost is higher, where f_2 always varies between 0–1.

4.3. Harmony search algorithm

Harmony search algorithm (HSA) [30, 32] is used to solve the optimisation problem mentioned in equation (46) because of its simplicity, less control parameters, strong balance of exploration and exploitation, and adaptability to different problem types. A good understanding of the working of the HSA comes from understanding its metaphoric origin in the principles of musicianship. During the composition of music, the composers start randomly with something similar to the required tunes and make adaptations or changes to the parts that were not required or the worst-case outcomes. The optimisation process begins by initialising the

Table 4. Component specifications.

Wind turbine	Solar PV	Battery	Biomass gasifier
Direct drive PMSG AC generator	Monocrystalline	Lead-acid battery	Rated capacity = 10 kW
Rated power = 5 kW	Rated power of PV panel = 5 kW/300 W_p	Rated capacity = 200 Ah	
Cut in speed (Vci) = 2.7 m s^{-1}	Open circuit voltage = 45.5 V	Rated voltage = 12 V	Operating for 12 h a day
Cut-out speed (Vco) = 25 m s^{-1}	Open circuit current = 8.64 A	Minimum SOC = 30%	
Rared power wind speed (Vr) = 11 m s^{-1}	$T_{stc} = 25^0$, G_{stc} = 1000 W m^{-2}	Maximum SOC = 100%	
Capital cost (Rs) = 5,00,000	Capital cost (Rs) = 3,50,000	Capital cost (Rs)15,000	
Maintenance cost (Rs) = 25,000	Maintenance cost (Rs) = 25,000	Maintenance cost (Rs) = 1,000	Capital cost (Rs) = 6,23,000
		Replacement cost (Rs) = 15,000	Maintenance cost (Rs) = 10,000

function with random values within the sample space. During each iteration, the algorithm evaluates the objective function and updates the worst-performing solutions based on the specified optimisation goal (minimisation or maximisation). The steps involved in the optimisation are given below.

Step 1: The parameters (HMS, PAR, HMCR) are initialised. HMS represents the harmony memory size, PAR represents the pitch adjustment rate, and HMCR represents the harmony memory consideration rate. These parameters are used while updating the solutions.

Step 2: The objective function values for the considered random harmony memory size will be evaluated.

Step 3: The worst harmony (solution) will be identified from the fitness values, and the worst harmony (solution) will be replaced by a better updated solution.

Step 4: Check for the convergence criteria or for the maximum number of iterations and return the optimal solution.

5. Simulation results and discussions

This study considers a rural village cluster as a case study. Solar irradiance, ambient temperature, and wind speed data for the location were obtained from the National Institute of Wind Energy (NIWE). Load demands of the village on an hourly basis were collected from the local substation. The efficiencies of the converters are 97% for the inverter and 95% for the rectifier. BESS is considered to supply the load for at least 30 min in the absence of power from renewables; therefore, four batteries are connected in series and 26 parallel paths. The biomass can be purchased from the locals at a price of Rs 0.30 kg^{-1}, and a total of 1.5 kg of biomass is required for producing 1 unit of energy. The grid purchase is limited to 10 kWh at a price of Rs 6 kWh^{-1} and the grid sale is limited to 18 kWh. The purchase limit from the grid is maintained to be low in order to make the design mainly depend on power generated from the HRES. The cost specifications for the preferred equipment are represented in table 4. For modelling the HRES, both the deterministic and probabilistic approaches are used, each with its own merits. The demerit of the deterministic approach is addressed by the probabilistic approach. For both approaches, the Harmony Search algorithm, implemented in MATLAB with a population size of 50, identified the optimal system configuration in approximately 10 seconds per 100-iteration run. The results from both approaches are presented in the following sections.

5.1. Deterministic approach

To identify the best possible combination of renewable energy sources for HRES, the optimization algorithm has been executed for different combinations in the deterministic approach. The renewable sources that are under consideration for modelling are solar PV, wind, and biomass. From these sources, the possible combinations (scenarios) that are considered for examination are:

1. Solar PV
2. Wind
3. Solar PV and wind
4. Wind and biomass

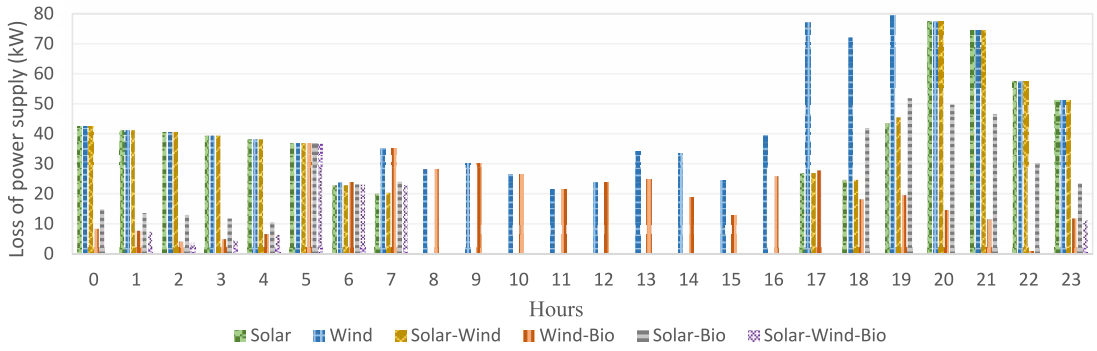

Figure 5. Loss of power supply for all the combinations.

Table 5. The optimal sizing of the renewable sources for different combinations with HSA.

Scenario	Algorithm	PV units (N_{pv})	Wind units (N_w)	Biomass units (N_{bio})	LPSP	LCOE (Rs.)
1	HSA	209	—	—	64%	7.6
2	HSA	—	10	—	48.7%	5.99
3	HSA	222	10	—	30%	5.34
4	HSA	—	18	3	15%	4.45
5	HSA	497	—	3	24%	5.11
6	HSA	317	15	3	5%	4.42

5. Solar PV and biomass
6. Solar PV, wind, and biomass

The optimal combination is selected based on the effectiveness of the model in achieving the objectives, its reliability in meeting load demand (quantified by LPSP), and its cost efficiency, determined by calculating the LCOE from the overall system cost. The results of different combinations employing the HSA algorithm with the weighted sum of LPSP and ALCC are shown in table 5. The table shows that among all possible renewable energy combinations for the HRES model, the PV-wind-biomass combination of the hybrid system delivered the best results in achieving lower costs and higher reliability (with minimal power supply loss). This configuration had an LPSP of 5% and a LCOE of Rs 4.42, significantly lower than the actual cost of Rs 6 per unit.

Notably, the combination of 317 PV units, 15 wind turbines, and 3 biomass units yields the lowest LCOE. This is because the LCOE is calculated from the net annual cost, which factors in both grid power purchases and sales. In this optimal scenario (Scenario 6), significantly more energy is sold to the grid than is purchased, and low-cost biomass is readily available. Conversely, other scenarios require substantial grid power purchases to meet demand, increasing their total cost and LCOE.

Figure 5 illustrates the daily loss of power supply for all the scenarios. Power loss is highest during the first and last seven hours of the day due to the absence of solar irradiance, leaving only wind and biomass to meet demand. During peak sunlight hours (10:00 am to 06:00 pm), solar generation eliminates power loss and produces a surplus used to charge the battery and sell to the grid. The biomass gasifier operates exclusively during the morning and evening peak load periods (the first and last six hours), which can be seen in the hourly LPSP trend. The bar graph demonstrates that power loss is highest across all system configurations during the first and last six hours of the day. At the 7th hour (06:00–07:00 am), the power loss is consistent for every combination. This uniformity occurs because solar generation remains unavailable due to a lack of irradiance, and the biomass gasifier, restricted to operating only during the initial and final six hours, is also inactive. Consequently, wind turbines alone must supply power during this interval.

Overall, the scenario relying exclusively on wind energy exhibits the greatest loss of power supply, peaking near 80 kW. This deterministic analysis identifies the hybrid combination of PV, wind, and biomass as the optimal system configuration, converging within 100 iterations (figure 6). It has been observed that the algorithm's initial guess (i.e., the best solution in the first iteration) often turns out to be reasonably close to the optimal solution, which is why the convergence appears close to the initial guess. However, it is important to note that this behavior may vary in another run. It should be noted, however, that this approach does not account for the inherent variability in renewable resources and load demand—a limitation addressed in the subsequent probabilistic analysis.

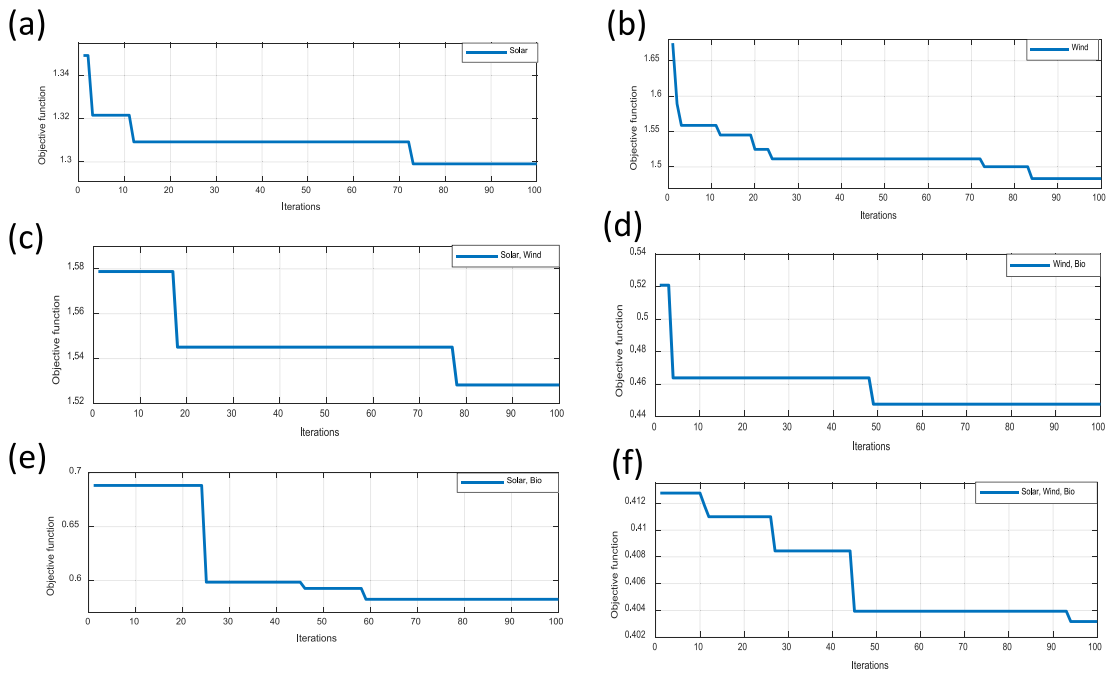

Figure 6. Convergence characteristics of HSA in (a) Scenario 1, (b) Scenario 2, (c) Scenario 3, (d) Scenario 4, (e) Scenario 5, and (f) Scenario 6.

5.2. Probabilistic approach

Even though the results from the deterministic approach are quite appreciable, the approach may not be practically adaptable because of its limitations in considering the variable nature of the renewables and load. While deterministic approaches offer simplicity and ease of implementation, they provide an incomplete picture of HRES performance due to the neglect of the variable nature of the renewables and load. Probabilistic methods, on the other hand, offer a more realistic and comprehensive understanding of HRES behaviour, leading to improved design, operation, and overall system optimisation for effective utilisation of renewable energy sources. The probabilistic approach is used to characterise the variable nature of the renewable sources as mentioned in section 2.2.

As mentioned in section 2.2, the Weibull PDF is used to model the solar irradiance and wind speed; similarly, the Normal PDF is used to model the load demand. The probabilistic approach can be done in two ways, which are:

i. Seasonal approach

ii. Monthly approach

The seasonal approach is the traditional way, and it has 4 typical estimated days for the 4 seasons of the year. The same estimated typical day parameters (wind speed, solar irradiance, and load) in a particular season are used for all days in that season. The seasons that are considered in this study are Winter (December, January, February), Summer (March, April, May, June), Monsoon (July, August, September), and Post-monsoon (October, November). In the monthly approach, there will be 12 typical estimated days, one for each month in a year. The same estimated typical day parameters, such as hourly solar irradiance, wind speed, and load, will be used for all the days in that month. For both monthly and seasonal approaches, the average optimal sizing of the HRES model is tabulated in table 6 along with the optimal sizing from the deterministic approach.

As shown in table 6, the probabilistic approach yields a more reliable system design, evidenced by a lower LPSP, than the deterministic method. Multiple simulation runs for both the monthly and seasonal approaches (tables 7 and 8) indicate that the seasonal strategy produces a superior optimal design, achieving a lower LCOE and LPSP. However, the practical adaptability of this seasonally-optimised design may be limited, as it relies on a single typical day to represent an entire season, potentially overlooking significant intra-seasonal variability. This could be answered by observing the results (optimal sizes) of exercising these optimal values on actual collected data, and seeing how close they match with the actual data. Tables 7 and 8 show the 10 optimal sizes of the designed HRES for the respective approaches (table 7 for the monthly approach and table 8 for the seasonal

Table 6. Optimal sizes of HRES for different approaches.

Approach	Algorithm	PV units (N_{PV})	Wind units (N_w)	Biomass gasifier units (N_{bio})	LPSP (%)	LCOE (Rs.)
Deterministic approach.	HSA	317	18	3	5	4.42
Probabilistic (Monthly approach)	HSA	305	20	3	2.23	4.52
Probabilistic (Seasonal approach)	HSA	264	19	3	2.25	4.45

Table 7. Optimal sizes of renewable sources for the monthly approach for 10 runs.

S. no	N_w	N_{pv}	N_{bio}	LPSP (%)	UC (Rs)	Grid sale (kWh year^{-1})	Grid purchase (kWh year^{-1})
1	17	354	3	2.52	4.51	37,568.39	10,340.65
2	18	349	3	2.27	4.52	41,257.30	8,573.47
3	17	356	3	2.49	4.51	37,785.51	10,241.29
4	19	280	3	2.85	4.5	38,345.51	13,200.34
5	19	314	3	2.36	4.51	42,074.91	9,828.74
6	18	350	3	2.25	4.52	41,367.87	8,545.27
7	18	298	3	3.01	4.49	36,102.19	13,056.78
8	18	341	3	2.39	4.51	40,318.58	9,004.79
9	18	365	3	2.05	4.54	42,901.62	7,993.01
10	20	305	3	2.23	4.52	45,664.24	8,547.23

Table 8. Optimal sizes of renewable sources for the seasonal approach for 10 runs.

S. no	N_w	N_{pv}	N_{bio}	LPSP (%)	UC (Rs)	Grid sale (kWh year^{-1})	Grid purchase (kWh year^{-1})
1	19	295	3	1.99	4.47	37,039.27	8,242.29
2	20	282	3	1.87	4.46	42,918.35	8,557.05
3	19	324	3	1.73	4.48	42,457.23	7,387.34
4	19	364	3	1.57	4.54	39,456.30	6,702.78
5	20	282	3	1.87	4.46	42,918.35	8,557.05
6	20	303	3	1.69	4.46	47,091.14	7,888.84
7	20	307	3	1.64	4.47	47,650.65	7,848.45
8	20	308	3	1.68	4.47	47,784.14	7,813.37
9	20	394	3	1.84	4.64	45,398.60	7,914.51
10	19	264	3	2.25	4.45	30,898.28	9,368.94

approach). These optimal sizes are tested on actual data (practical one-year data), and the observations are tabulated in tables 9 and 10.

In tables 9 and 10, the ABS of LPSP represents the absolute difference between the LPSP obtained when the same optimal sizes are applied to actual data and with respect to the proposed approach. Similarly, MSE represents the mean squared error of the absolute error. For the monthly approach, the best optimal sizing for modelling of HRES is 20 wind units, 305 PV units, and 3 biomass units, which gives the LPSP percentage as 2.23 and UC as Rs 4.52 per kWh. But the same optimal sizing values for the actual yearly data give the LPSP percentage as 3.24 and UC as Rs 4.49 per kWh. Similarly, from the seasonal approach for the best optimal sizing of 264 PV units, 19 wind units, and 3 biomass units gives the LPSP as 2.25% with UC as Rs 4.45, but the same sizing when applied on the actual data gives the LPSP as 4.41% with Rs 4.43 per LCOE. It says that for both approaches, there is a shift in LPSP values if the sizing is used on actual data. The monthly approach (table 9) has less MSE value compared to the MSE in the seasonal approach (table 10), which suggests that the power generated from the monthly approach is well inclined towards the actual yearly power production of the sources compared to the seasonal approach. Therefore, the optimal sizes obtained from the monthly approach are more adaptable practically.

The daily power generation profiles for selected months, utilizing the optimal system sizing determined by the monthly approach, are shown in figures 7–9. The trends for

December (figure 7) indicate periods of reduced solar irradiance and moderate wind speeds, leading to moderate generation levels (solar PV peaking at 62 kW; wind at 40 kW). During hours 5th–10th, the concurrent unavailability of biomass energy and lower solar generation necessitate purchasing up to 10 kW from the grid,

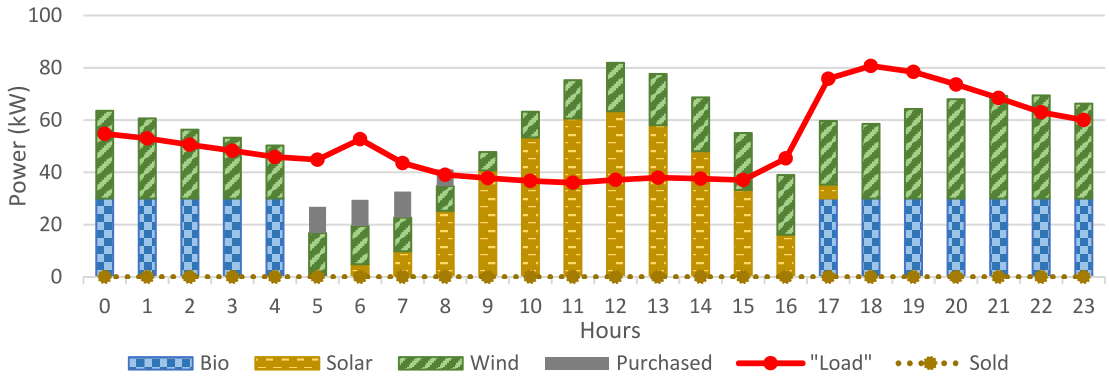

Figure 7. Load demand and power generation trends in a day of December month.

Table 9. Results of the use of optimal sizing from monthly approach on actual collected yearly data.

S. no	N_w	N_{pv}	N_{bio}	LPSP (%)	UC (Rs)	Grid sale (Kwh year^{-1})	Grid purchase (Kwh year^{-1})	ABS of LPSP (%)	MSE of LPSP (%)
1	17	354	3	3.79	4.47	46,914.83	12,722.68	1.27	1.6129
2	18	349	3	3.4	4.49	50,422.82	11,573.75	1.13	1.2769
3	17	356	3	3.76	4.48	47,132.22	12,628.64	1.27	1.6129
4	19	280	3	4.09	4.44	47,904.30	14,367.68	1.24	1.5376
5	19	314	3	3.4	4.47	50,951.88	12,107.39	1.04	1.0816
6	18	350	3	3.39	4.49	50,554.35	11,526.71	1.14	1.2996
7	18	298	3	4.23	4.44	45,605.29	14,612.60	1.22	1.4884
8	18	341	3	3.51	4.48	49,600.74	11,963.90	1.12	1.2544
9	18	365	3	3.19	4.51	52,268.34	10,952.17	1.14	1.2996
10	20	305	3	3.24	4.49	54,115.00	11,297.62	1.01	1.0201
								=11.58	=1.3484

Table 10. Results of the use of optimal sizing from the seasonal approach on actual collected yearly data.

S. no	N_w	N_{pv}	N_{bio}	LPSP (%)	UC (Rs)	Grid sale (kWh year^{-1})	Grid purchase (kWh year^{-1})	ABS of LPSP (%)	MSE of LPSP (%)
1	19	295	3	3.81	4.45	49,198.77	13,297.96	1.82	3.3124
2	20	282	3	3.61	4.47	51,905.32	12,774.20	1.74	3.0276
3	19	324	3	3.33	4.48	51,946.74	11,561.40	1.6	2.56
4	19	364	3	2.8	4.53	56,333.05	9,828.29	1.23	1.5129
5	20	282	3	3.61	4.47	51,905.32	12,774.20	1.74	3.0276
6	20	303	3	3.28	4.49	53,911.23	11,393.39	1.59	2.5281
7	20	307	3	3.21	4.49	54,321.87	11,209.87	1.57	2.4649
8	20	308	3	3.19	4.49	54,425.84	11,162.11	1.51	2.2801
9	20	394	3	2.25	4.61	63,561.81	7,858.00	0.41	0.1681
10	19	264	3	4.41	4.43	46,553.53	15,678.09	2.16	4.6656
								=15.37	= 2.554

reducing grid sales to nearly zero. The daily operation for August and March, shown in figures 8 and 9, respectively, demonstrate the ability of the system to minimize grid dependency. In August (see figure 8), high wind speeds lead to significant wind generation, supplemented by moderate solar PV output. This surplus allows the system to sell power to the grid from the 7th hour onward, eliminating the need for purchases. Conversely, March (see figure 9) features very high solar irradiance, with PV generation peaking at 80 kW. In both cases, the HRES effectively meets the load with minimal grid reliance. To maximise the utilisation of renewable energy and minimise grid dependency, the optimisation process constrained grid power exchange to a purchase limit of 10 kW and a sales limit of 18 kW. The role of change in the grid sale capacity has a significant effect on the amount of energy generated from each of the sources. As shown in figure 10, increasing the grid sales capacity does not affect power generation from the biomass gasifier but results in a higher contribution from the PV and wind turbine units.

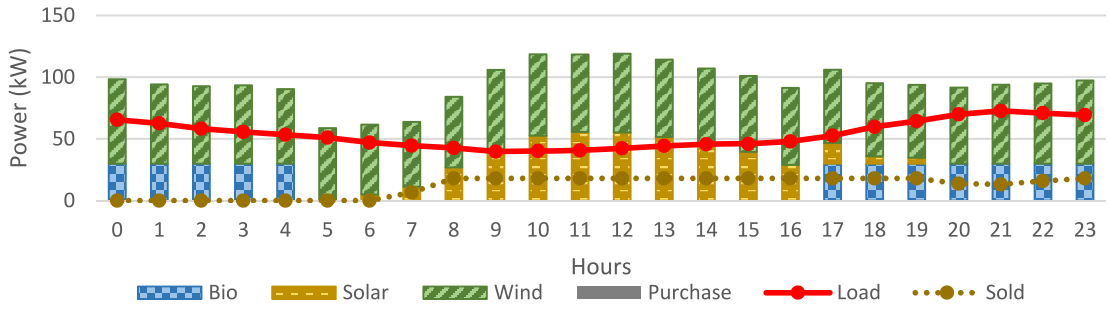

Figure 8. Load demand and power generation trends in a day of August month.

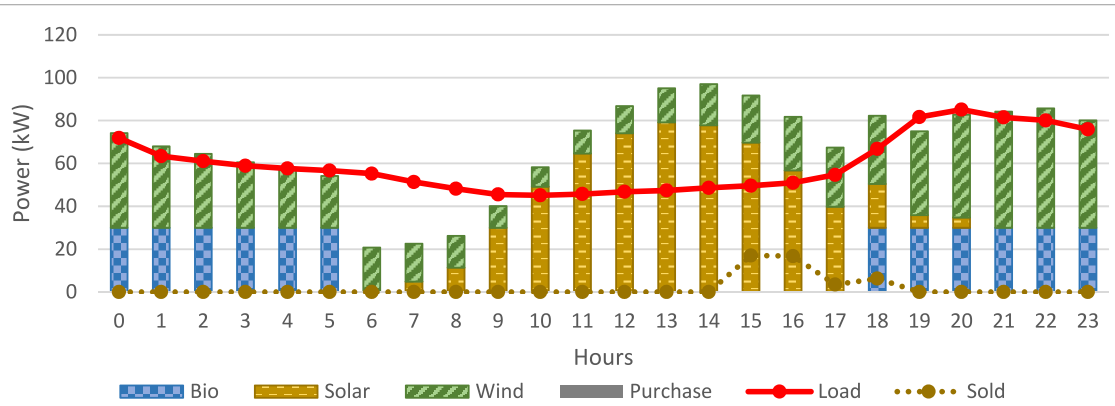

Figure 9. Load demand and power generation trends in a day of March month.

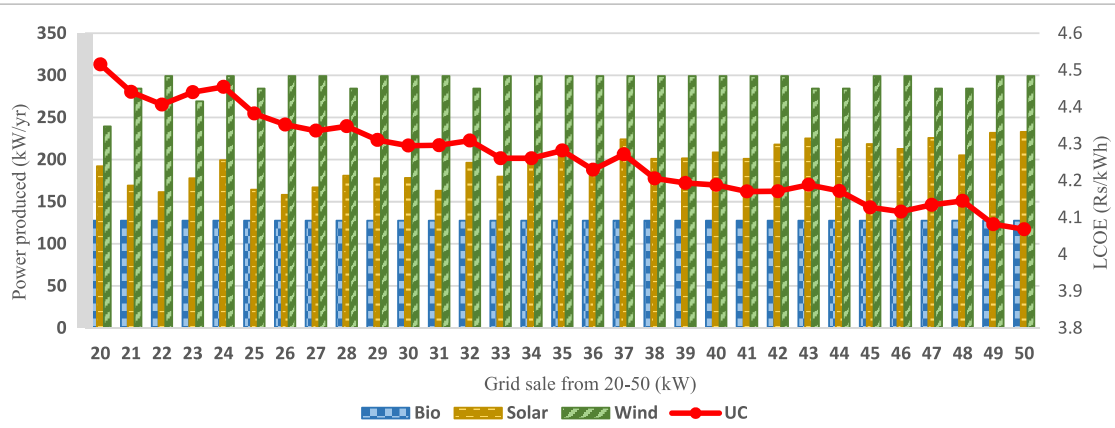

Figure 10. Effect of grid sale capacity on solar and wind power production and UC.

5.3. Comparative assessment

The proposed monthly probabilistic methodology was evaluated against both standard deterministic techniques [6, 8, 11, 21, 25] and a comparative seasonal probabilistic model. The results, tabulated in table 6, demonstrate superior performance of the proposed approach in achieving a lower Levelized Cost of Energy (LCOE) and an improved reliability metric (LPSP) compared to deterministic approach. While its overall cost and reliability results are comparable to the seasonal model, an analysis in section 5.2 (see tables 7, 8, and 9) confirms that the monthly variations model yields outcomes that align more closely with practical recorded data. As mentioned in table 11, this work provides a significant advance beyond the referenced studies [6, 8, 11] by incorporating a diverse mix of renewables, uniquely modelling the stochastic nature of both generation and load probabilistically, moving beyond the sole use of historical data [6, 8, 11, 21, 25] and introducing a rigorously sized HRES based on the EPRI handbook. Furthermore, it offers a novel economic analysis of grid interaction, uncovering a previously unreported trade-off whereby increased grid sales capacity reduces LCOE

Table 11. Comparative assessment.

Parameter	[6]	[8]	[11]	[21]	[25]	Proposed
Renewables considered	Solar, Wind	Solar, Wind, Diesel Generator	Solar, Wind, Diesel Generator	Solar, Wind, Fuel cells	Solar, Wind, Biomass	Solar, Wind, Biomass
Addressed the Stochastic nature of RE?	No	No	No	No	No	Yes
Addressed load variations?	No	No	No	No	No	Yes
Grid integrated?	Yes	No	No	Yes	Yes	Yes
Effect of Grid participation included?	No	No	No	No	No	Yes
Energy Storage included?	Yes	No	Yes	Yes	Yes	Yes
Optimisation Technique used	Meta-heuristic optimisation	DIRECT algorithm	Ant colony optimisation	Fuzzy logic-GWO	HOMER	HSA
Objective functions	Cost, LPS	Cost, LPS	Cost, LPS	Cost, Energy management	Cost	LCOE, LPSP

but can lead to renewable sources oversizing. The proposed approach was compared against the commercial HOMER software trial version (see supplementary document). The observed discrepancy is likely due to the limited optimisation precision of the trial software. However, it shows our method provides a more tailored and cost-effective sizing methodology.

6. Conclusion

This study proposes an optimal design methodology for a hybrid renewable energy system (HRES) to enhance reliability while minimising the unit energy cost. The system was designed for a hamlet with a peak load of 100 kW, incorporating solar PV, wind, and biomass energy sources. Simulation results from a deterministic analysis identified the hybrid combination of solar, wind, and biomass as the most effective configuration, offering high reliability and low cost. To account for the inherent variability in renewable resources and load, probabilistic modelling using Probability Density Functions (PDFs) was employed. A Weibull distribution was used to model solar irradiance and wind speed, while a normal distribution best represented the load profile. The probabilistic approach improved system reliability, with a monthly variation model outperforming a seasonal model in terms of alignment with actual recorded annual data. Using the monthly approach, the optimally sized HRES achieved a Loss of Power Supply Probability (LPSP) of 2.23% and a LCOE of Rs. 4.52 per kWh, results which closely match practical annual data. Furthermore, increasing the grid sales capacity from 20 kW to 50 kW reduced the LCOE, demonstrating the impact of grid exchange policies on overall system economics. This study could be further extended to a probabilistic framework to optimise HRES design for multi-objectives, such as minimising emissions and maximising grid independence, while also exploring machine learning techniques for more accurate forecasting of renewable generation and load.

Declarations

All the authors are contributed equally for this manuscript.

Ethical approval

Not applicable.

Funding

Not applicable.

Conflict of interest

The authors do not have any known conflicts of interest.

Data availability statement

All data that support the findings of this study are included within the article (and any supplementary files).

Author contributions

Ravindra Kollu 0000-0002-3936-3365
Methodology (equal), Supervision (equal), Validation (equal), Writing – review & editing (equal)

References

[1] Press Information Bureau (PIB) 2025 https://pib.gov.in/PressNoteDetails.aspx?NoteId=153279&ModuleId=3
[2] Zhang J 2024 Energy access challenge and the role of fossil fuels in meeting electricity demand: promoting renewable energy capacity for sustainable development *Geoscience Frontiers* **15** 101873
[3] Niyogi A, Sarkar P, Bhattacharyya S, Pal S and Mukherjee S 2024 Harnessing the potential of agriculture biomass: reuse, transformation and applications in energy and environment *Environ. Sci. Pollut Res.* **32** 19180–203
[4] Mlilo N, Brown J and Ahfock T 2021 Impact of intermittent renewable energy generation penetration on the power system networks —a review *Technol Econ Smart Grids Sustain Energy* **6** 25

[5] Bassey K E 2023 Hybrid renewable energy systems modelling *Engineering Science & Technology Journal* **4** 571–88
[6] Hossain Lipu M S, Rahman M S A, Islam Z U, Rahman T, Rahman M S, Meraj S T, Hossain M Y and Mansor M 2025 Review of energy storage integration in off-grid and grid-connected hybrid renewable energy systems: structures, optimizations, challenges and opportunities *Journal of Energy Storage* **122** 116629
[7] Balamurugan P, Ashok S and Jose T L 2009 Optimal operation of Biomass/Wind/PV hybrid energy system for rural areas *Int. J. Green Energy* **6** 104
[8] Belfkira R, Zhang L and Barakat G 2011 Optimal sizing study of hybrid wind/PV/diesel power generation unit *Sol. Energy* **85** 100
[9] Abbes D, Martinez A and Champenois G 2012 Eco-design optimisation of an autonomous hybrid wind photovoltaic system with battery storage *IET Renewable Power Gener* **6** 358–71
[10] Sharafi M and EL Mekkawy T Y 2014 Multi-objective optimal design of hybrid renewable energy systems using PSO-simulation based approach *Renew able Energy* **68** 67–79
[11] Suhane P, Rangnekar S, Mittal A and Khare A 2016 Sizing and performance analysis of standalone wind photo voltaic based hybrid energy system using ant colony optimisation *IET Renewable Power Gener.* **10** 964
[12] Razmi H, Hasan D-M and Olamaei J 2020 Comparative study of optimization algorithms for sizing of Wind Turbine/Fuel Cell/Electrolyzer/Hydrogen Tank in the hybrid stand-alone power system *Signal Processing and Renewable Energy* **4** 81–94 (https://oiccpress.com/spre/article/view/7827)
[13] Menesy A S, Sultan H M, Habiballah I O, Masrur H, Khan K R and Khalid M 2023 Optimal configuration of a hybrid photovoltaic/wind turbine/biomass/hydro-pumped storage-based energy system using a heap-based optimization algorithm *Energies* **16** 3648
[14] Koholé Y W, Wankouo Ngouleu C A, Fohagui F C V and Tchuen G 2024 Optimization of an off-grid hybrid photovoltaic/wind/diesel/fuel cell system for residential applications power generation employing evolutionary algorithms *Renew. Energy* **224** 120131
[15] Kyritsis A, Voglitsis D, Papanikolaou N, Tselepis S, Christodoulou C, Gonos I and Kalogirou S A 2017 Evolution of PV systems in Greece and review of applicable solutions for higher penetration levels *Renew. Energy* **109** 487–99
[16] Cao J, Du W, Wang H and McCulloch M 2018 Optimal sizing and control strategies for hybrid storage system, as limited by grid frequency deviations *IEEE Trans. Power Syst.* **33** 5486
[17] Thapa S and Karki R 2016 Reliability benefit of energy storage in wind inte grated power system operation *IET Gener. Transm. Distrib.* **10** 807–14
[18] Khalid M and Savkin A V 2010 A model predictive control approach to the problem of wind power smoothing with controlled battery storage *Renew. Energy* **35** 1520–6
[19] Mears L D and Gotschall H L 2004 Wind applications for benefit-cost assessments. in EPRI—Handbook supplement of energy storage for grid connected wind generation applications *Technical Update* 3–9(EPRI)
[20] Basaran K, Cetin N S and Borekci S 2017 Energy management for on-grid and off-grid wind or PV and battery hybrid systems *IET Renewable Power Gener.* **11** 642–9
[21] EI-Bidairi K S, Nguyen H D, Jayasinghe S D G and Mahmoud T S 2018 Multi-objective intelligent energy management optimization for grid-connected microgrids *2018 IEEE International Conference on Environment and Electrical Engineering and 2018 IEEE Industrial and Commercial Power Systems Europe (EEEIC / I&CPS Europe)* (Italy) 1–6
[22] Tayab U B and Yang F 2018 Energy management system for a grid-connected microgrid with PV and battery energy storage system *Aus tralian & New Zealand Control Conf. (ANZCC)* (Melbourne, VIC) 141–4
[23] Elgammal A and El-Naggar M 2018 Energy management in smart grids for the integration of hybrid wind-PV-FC-battery renewable energy resources using multi-objective objective particle swarm optimization *J. Eng* **2018** 1806–16
[24] Alluraiah N C and Vijayapriya P 2023 Optimization, design, and feasibility analysis of a grid-integrated hybrid AC/DC microgrid system for rural electrification *IEEE Access* **11** 67013–29
[25] Kurukuri P, Mohamed M R, Raavi P H and Arya Y 2024 Optimal planning and designing of microgrid systems with hybrid renewable energy technologies for sustainable environment in cities *Environ Sci Pollut Res* **31** 32264–81
[26] Reddy B K, Giri N C, Yemula P K, Agyekum E B and Arya Y 2024 Optimal operation of cogeneration power plant integrated with solar photovoltaics using DLS-WMA and ANN *Int. J. Energy Res.* 5562804 16 pages **2024**
[27] Kollu R, Rao R S and Narasimham S V L 2012 Wind distribution analysis incorporating artificial bee colony algorithm *Int. Conf. on Advances in Power Conversion and Energy Technologies (APCET), Mylavaram, India* 1–6
[28] Kollu R, Rayapudi S R, Narasimham S and Pakkurthi K M 2012 Mixture probability distribution functions to model wind speed distributions *Int. J. Energy Environ, Eng.* **3** 27
[29] Villanueva D, Pazos J L and Feijoo A 2011 Probabilistic load flow including wind power generation *IEEE Trans. Power Syst.* **26** 1659–67
[30] Pan Q K *et al* 2010 A self-adaptive global best harmony search algorithm for continuous optimization problems *Appl. Math. Compute.* **216** 830–48
[31] Li X, Tian Z, Wu X, Feng W and Niu J 2024 Optimal planning for hybrid renewable energy systems under limited information based on uncertainty quantification *Renew. Energy* **237** 121866
[32] Wang J, Ouyang H, Zhang C, Li S and Xiang J 2023 A novel intelligent global harmony search algorithm based on improved search stability strategy *Sci Rep.* **13** 7705